24th INTERNATIONAL CONGRESS ON SOUND AND VIBRATION
23–27 July 2017, London

EXPERIMENTAL MAXIMISATION OF THE POWER ABSORBED BY AN INERTIAL ACTUATOR FOR STRUCTURAL VIBRATION CONTROL

Stefano Camperi, Maryam Ghandchi-Tehrani and Stephen J. Elliott
Institute of Sound and Vibration Research, University of Southampton, Highfield, Southampton, UK
email: s.camperi@soton.ac.uk

This paper presents the experimental results of a velocity feedback control of a vibrating plate, excited by a random point force. The control unit consists of a sensor collocated with an inertial actuator. The inertial actuator is driven with a current proportional to the measured velocity of the structure.

For this control system, an optimal feedback gain exists, which minimises the time-averaged kinetic energy of the global structure. By increasing the gain beyond the optimal gain, the performance of the active control system does not improve and the feedback is less effective, since the boundary conditions can change due to the pinning.

In order to define an equivalent performance estimator, which can be locally measured, the time-averaged power absorbed by the inertial actuator for different values of feedback gain is investigated.

In this study, a frequency-domain analysis of the control system is presented. A load cell is added between the structure and the actuator, so that the control force generated by the control unit can be measured, and hence the power absorbed can be estimated. It is shown that, as the feedback gain increases, the time-averaged power absorbed increases to a maximum value, whereas the local velocity of the structure decreases.

1. Introduction

Inertial actuators for structural vibration reduction are an attractive solution when active feedback control is required. They can be directly attached to the structure without the need of external supports, and driven with an electrical feedback signal proportional to the velocity of the structure.
A common solution is a local control unit, in which actuator and sensor are collocated, so that the conditional stability is maximised [1, 2]. In general, the increase of the feedback gain guarantees the local reduction of the plate vibration at the sensor position; therefore, large reductions can be obtained mounting the control unit close to the main disturbance source. However, for multiple disturbance sources, the minimisation of the local velocity at the control position does not correspond to a global reduction of the level of vibration in the structure [3]. The optimal feedback gain, which gives the best global control, depends on the type of excitation; the structure mobility; and the actuator dynamics.
Adaptive control allows finding this optimal feedback gain through a performance estimator. Elliott et al. [1] have shown that, for an unconditionally stable control system excited with a white-noise, the minimisation of the time-averaged kinetic energy almost corresponds to the maximisation of the local power absorbed by the actuator. Therefore, the control unit can self-tune its feedback gain in order to minimise the power absorbed by the actuator [4].

This paper is concerned with the experimental measurement of the time-averaged power absorbed by an inertial actuator from a rectangular plate excited by a broadband point force. An analytical model of the system has been previously presented in an another paper by the author [2]. In contrast with previous studies, the control force is directly measured accounting for both passive and active effects, and it is used to measure the power absorbed. In the first section, the experimental set-up is presented. Then, the open-loop stability of the control system is analysed considering the effect of every single component of the feedback-loop [4, 5]. Finally, the performance of the control system is investigated both in terms of local vibration reduction and power absorbed.

2. Experimental set-up

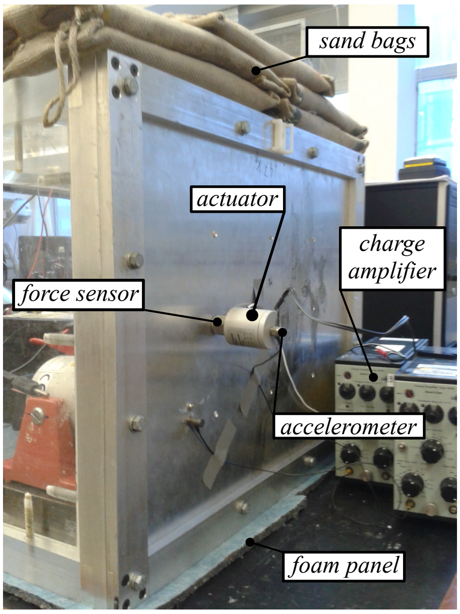

(a)

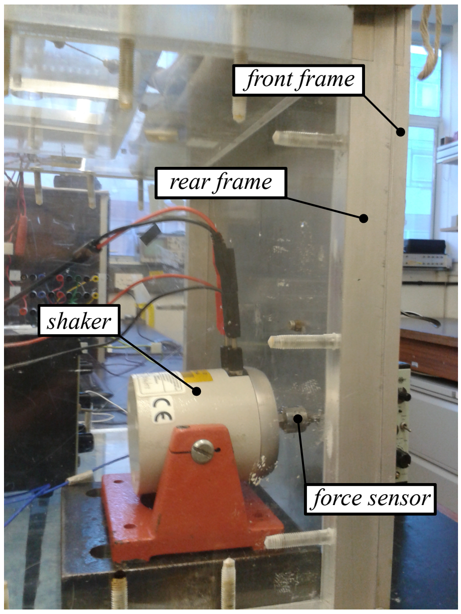

(b)

Figure 1: Experimental set-up: (a) front view of the clamped plate with the collocated actuator and accelerometer; (b) rear view of the plate with the clamping frames and the primary source.

The structure considered in this study is a rectangular aluminium plate excited by a white-noise point source generated by a shaker LDS-V200. As shown in Fig. 1a, the control unit consists of an accelerometer and an inertial actuator pair collocated, mounted on the plate. In addition, a force sensor PCB-208C01 is placed between the actuator and the plate, so that the force transmitted by the actuator to the structure can be measured.
The positions of the primary excitation and the control unit, as well as the geometrical and physical properties of each component are summarised in Table 1.
As shown in Fig. 1b, the plate is clamped between two aluminium frames of different thickness: 25 mm the rear one, and 10 mm the front one. The frames have been screwed together with a torque key, in such a way that the boundary conditions are as uniform as possible along the perimeter of the plate. The clamping frame is mounted on a side of a Perspex box, which is left open to avoid coupling between the panel and the volumetric modes of the cavity. The dynamic coupling between the plate and the box can be neglected, as the Perspex is a highly damped material. In order to reduce the ground noise a foam panel has been added underneath, and sand bags on the top to lower possible resonances of the test-rig.
A scheme of the control unit is presented in Fig. 2. The charge output of the piezoelectric accelerometer B&K-4375 is amplified via a charge amplifier B&K-2635, and sent to the digital platform

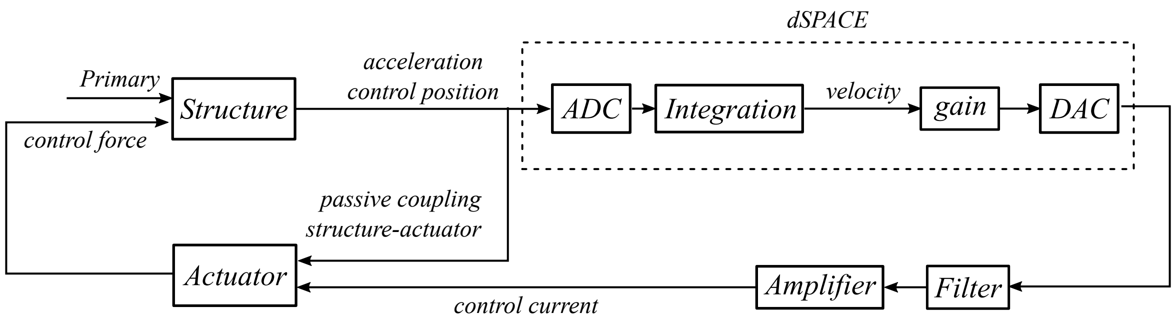

Figure 2: Schematic representation of the control system.

dSPACE running with a sampling frequency f_s of 16 kHz. Numerical integration is performed in order to obtain a velocity signal. A second order Butterworth digital high pass filter is designed, to avoid numerical amplification of the signal at low frequency due to integration, with a cut-off frequency of 3 Hz. A control signal proportional to the velocity by means of a gain g is generated; filtered to avoid aliasing effects; amplified through a Micromega PR-052-01-04-03 amplifier; and finally fed-back into the inertial actuator as current. The control force generated by the actuator has a passive component due to the coupling between the structure and the actuator, and an active component generated by the current flowing through the coils [6, 7].

Table 1: Physical properties of the plate and inertial actuator

	Parameter	Value
Aluminium panel	Dimension (mm^2)	412×312
	Thickness (mm)	1
	Density (kg/m^3)	2700
	Young's modulus (GPa)	70
	Poisson ratio (GPa)	0.33
	Shaker position (x_p, y_p)(mm)	(65,93)
Inertial actuator Micromega IA01	Moving mass (g)	32
	Base mass (g)	53
	Natural frequency (Hz)	8.7
	Damping ratio	0.4
	Voice coil coefficient (N/A)	1.6
	Electrical resistance (Ω)	3
	Electrical inductance (mH)	0.1
	Actuator position (x_c, y_c) (mm)	(103,156)

3. Open-loop stability

In order to assess the stability of the control system, the Nyquist Criterion is applied to the open-loop transfer function between the signal from the dSPACE and the velocity measured by the sensor. Theoretically, the conditional stability is determined by the phase-shift in the force transmitted by the inertial actuator below its resonance, which makes the control force to be in-phase with the structure response. However, in a real system other two sources of delay can be identified: the analogue devices such as filters and amplifiers, and the digital operations such as sampling, filtering and integration.

In this section, according to Fig. 2, the effect of each component of the feedback loop on the overall stability is analysed separately.

The measured FRF of the Micromega amplifier is shown in Fig. 3a. The amplifier has a fixed gain

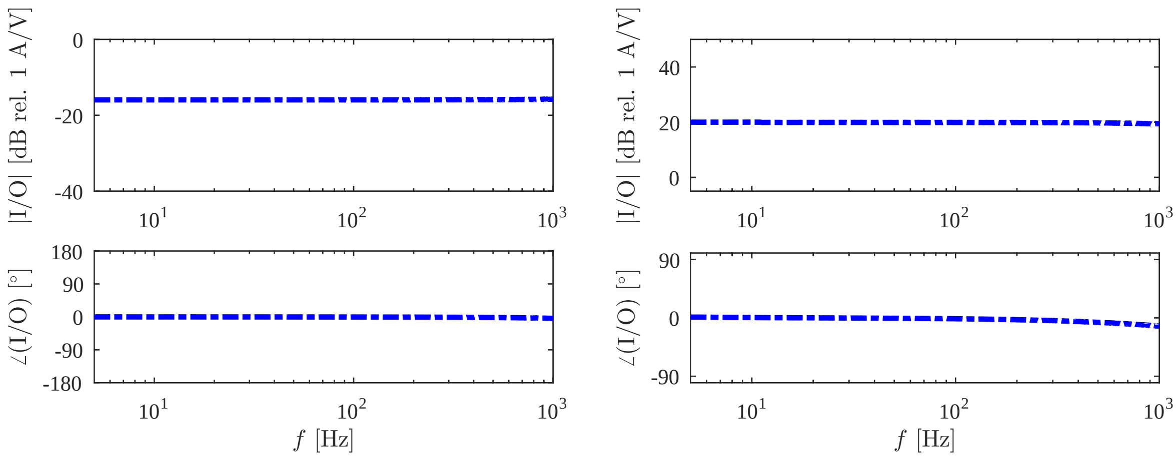

(a) (b)

Figure 3: Measured FRFs of (a) the amplifier, and (b) the analogue filter.

between the input voltage and the output current, whose amplitude is constant in the frequency range considered, as well as its phase.

The cut-off frequency of the low-pass filter has been set to be equal to the sampling frequency to avoid aliasing. The FRF between input and output voltage is almost constant at all the frequencies shown in Fig. 3b.

In order to have a better understanding of the active force generated by the inertial actuator when

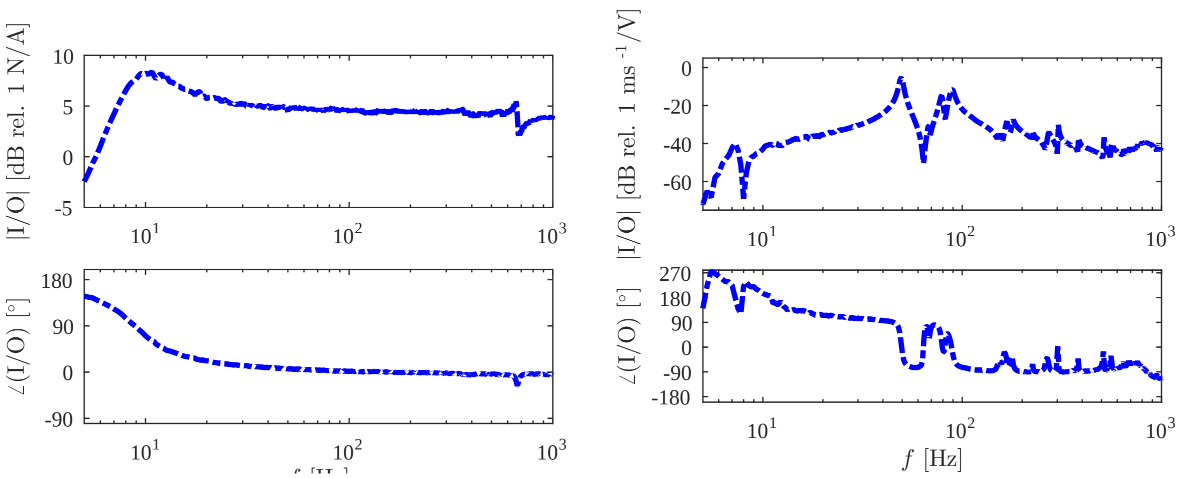

(a) (b)

Figure 4: Measured FRFs of (a) the blocked force of the inertial actuator with respect to the input current, and (b) the velocity of the plate at the control position with repect to the actuator driving current.

current driven, the force generated by the inertial actuator on a fixed ground has been plotted in Fig. 4a. The fixed ground in this experiment allows the passive coupling structure-actuator, shown in Fig. 2, to be neglected; and so the actuator dynamics can be investigated independently from the structure. In the frequency range above the natural frequency, the inertial actuator behaves as an ideal force source, which is in phase with the driving current, and with amplitude proportional to the voice coil coefficient. A second peak can be noticed around 650 Hz, which is assumed to be due to internal

resonant effects. Conversely, below the natural frequency, the force is in opposite phase with respect to the driving current. Therefore, in a velocity feedback control, the force generated by the inertial actuator below its resonance is in phase with the velocity of the structure, and thus the feedback loop is only conditionally stable.
When the inertial actuator is mounted on a plate, its dynamics couples with the structure, as shown in Fig. 4b. The structural response is characterised by well separated peaks in correspondence with the resonances of the structure. However, a further peak can be noticed around 7 Hz, due to the coupling between the inertial actuator and the structure. The sensor and the actuator are collocated, therefore the phase of the mobility is bounded between $90°$ and $-90°$ at almost all frequencies. Nevertheless, because of the phase shift discussed in Fig. 4a, the phase converges to $270°$ decreasing the frequency below the first structural resonance. Finally, at high frequencies, the phase drops below $-90°$ because of the digital filtering and integration. The sensor is placed on the inertial actuator case, which can be assumed rigid in the frequency range considered, and any significant difference has been noticed with the accelerometer fixed directly on the plate.
The noise in the measured results at low frequencies is due to the dynamic characteristic of the actuator. As shown in Fig. 4a, the force transmitted in the frequency range below the resonance drops dramatically. Moreover, in this region the response of the structure is controlled by the stiffness, so the mechanical impedance seen by the inertial actuator approaches the fixed ground condition. Finally, the finite stroke of the moving mass imposes a limit on the driving current.
The stability of the feedback loop depends on the coupling between the actuator and the structure. Because of the phase shift in the force transmitted by the actuator below its resonance, the stability of the feedback loop can be improved using an actuator highly damped, and with a natural frequency well below the resonances of the structure. Figure 5 shows a comparison between the measured

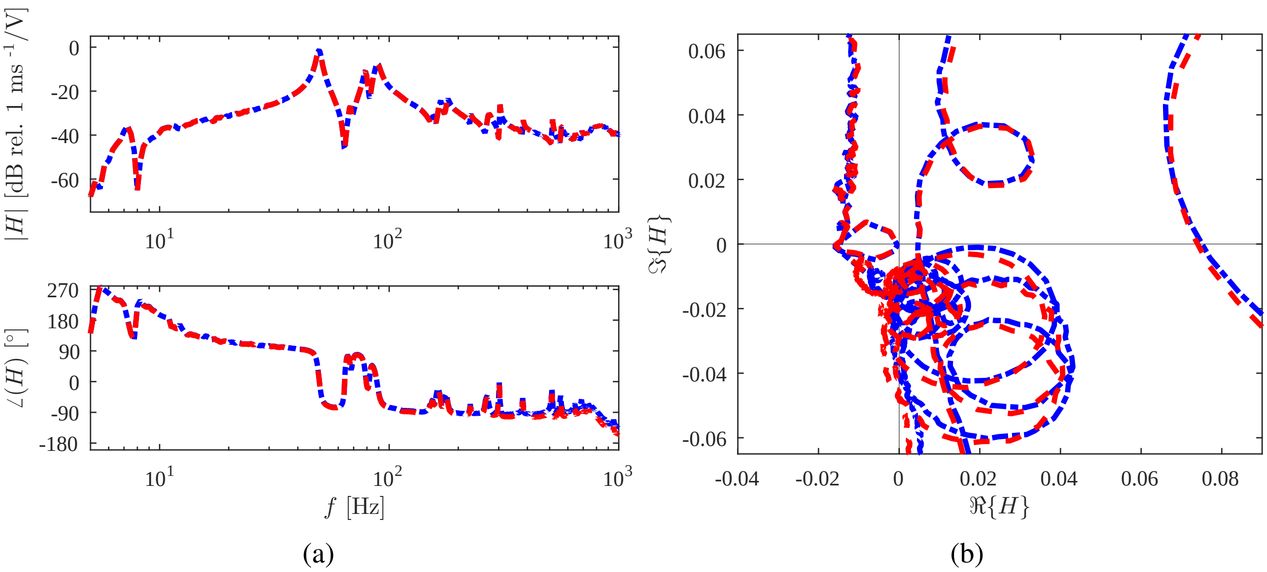

Figure 5: Comparison between the measured open-loop FRF (blue line) and the predicted one using the individual measured responses of each element of the feedback-loop (red line). (a) Bode plot, (b) Nyquist plot.

open-loop FRF, and the predicted one using the individual measured responses of each element of the feedback-loop. The results are in good agreement over all the frequency range considered. The phase-delay in the high-frequency range is due to the 'sample and hold' of the input signal from the dSPACE, which introduces a delay proportional to the digital sampling frequency.
The stability limit of the control loop can be derived from the Nyquist plot of the open-loop FRF, as shown in Fig. 5. In particular, the gain limit is defined as the inverse of the minimum distance between the intersection of the FRF with the real axis and the point (-1,0). On the one hand, the resonance

of the inertial actuator couples with the structural response making the FRF turn in anti-clockwise direction. From Fig. 5b, the closer the natural frequency of the inertial actuator to a structural resonance, the greater the circle shifted in the left-hand side of the Nyquist plot, and therefore the smaller is the stability limit. On the other hand, the digital sampling frequency delay makes the FRF to rotate in clockwise direction: the smaller is the sampling frequency, the larger is the number of structural resonances shifted on the left hand side.
As shown in Fig. 5b, the stability of the control system can be improved with a high sampling frequency and using an inertial actuator whose natural frequency is well below the structural resonances.

4. Control system

In the closed-loop system, the plate is excited by a primary point-force generated by a shaker driven with a white-noise voltage. In order to reduce the plate vibration, the inertial actuator is driven with a current proportional to the local velocity of the plate.
The mobility of the plate at the control position with respect to the primary excitation is shown in Fig.

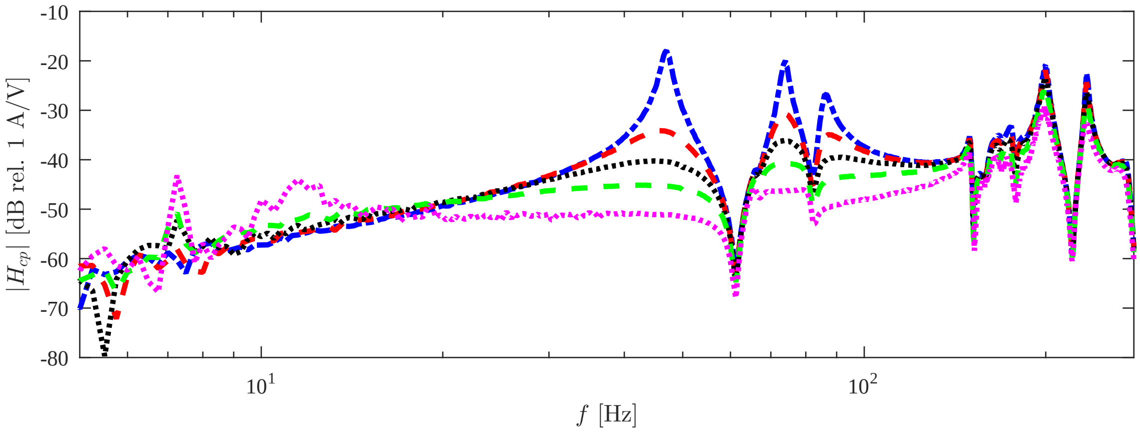

Figure 6: Mobility of the plate at the control position with respect to the primary excitation for different values of feedback gain: $g = 0\%$ in blue line; $g = 0.05\%$ in red; $g = 0.11\%$ in black; $g = 0.20\%$ in green; $g = g_{lim}$ in pink.

6 for different values of feedback gain. When there is no feedback signal, the mobility is characterised by well separated and sharp peaks due to the small structural damping. Increasing the feedback gain, a good reduction of the first resonances can be achieved, up to -30 dB for the first mode. However, because of the phase-shift in the force transmitted by the inertial actuator below its resonance, the mobility in the low frequency range is magnified when the feedback gain rises. In particular, above a certain feedback gain, a smooth peak starts growing in amplitude and moving down in frequency, until it reaches the inertial actuator resonance, where the system becomes unstable.
The noise in the results in the low-frequency range is due, on the one hand, to the primary excitation which, because of the primary amplifier, does not excite properly the low frequecies. On the other hand, it is believed that non-linear phenomena occur in the inertial actuator when the gain is increased. In the high frequency range, results have not been plotted above 280 Hz, as the control has no effect on the higher structural modes.
However, the local reduction of the plate velocity does not guarantee good global performance. Indeed, the vibration level at other points of the structure might be actually magnified. In order to achieve a global control, previous studies have looked at the minimisation of the kinetic energy of the structure. Moreover, it has been shown that, for an unconditionally stable control system, the minimisation of the kinetic energy almost corresponds to the maximisation of the power absorbed. The time-averaged power absorbed by the inertial actuator from the structure can be directly obtained

from the velocity and force signals as time-averaged value over N samples as

$$\bar{P} = -\frac{1}{N}\sum_{n=1}^{N} f_c(\Delta n) v_c(\Delta n) \tag{1}$$

where $f_c(\Delta n)$ and $v_c(\Delta n)$ are, respectively, the control force transmitted by the inertial actuator to the plate, and the velocity of the plate at the control position at the time n/f_s, where f_s is the sampling frequency.

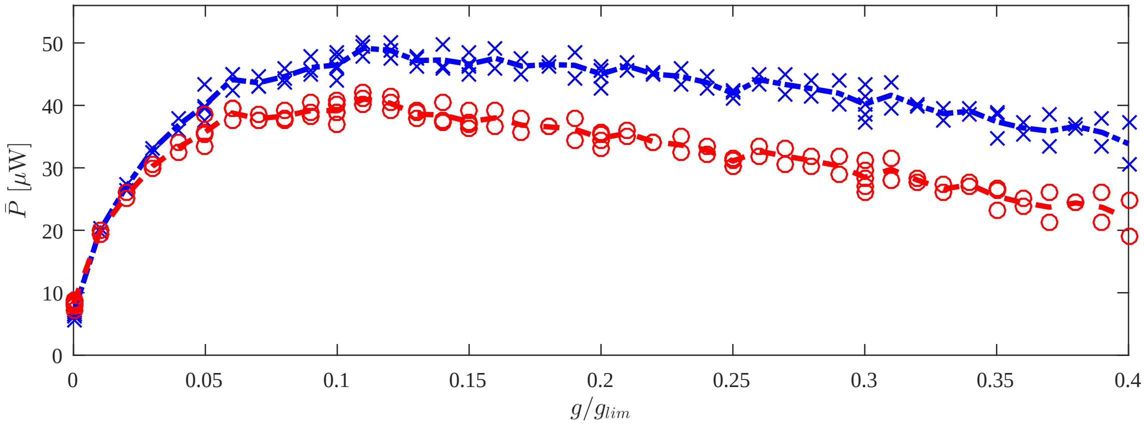

Figure 7: Measured time-averaged power absorbed by the inertial actuator from the structure: in blue the time integration, in red the time integration of the filtered signals.

The time-averaged power absorbed is shown in Fig. 7, where the feedback gain has been normalised with respect to the gain limit. When the feedback signal is zero, the inertial actuator can be described as a simple mechanical impedance, and the power absorbed is dissipated by the damper. However, as soon as the feedback gain is increased, the power absorbed rises dramatically up to a maximum, which is experimentally measured at 11% of the gain limit.

Beyond the maximum, the power absorbed starts decreasing up to the stability limit. This is due to the enhancement of the vibration in the low frequency range by the inertial actuator. In particular, because of the phase-shift in the force transmitted by the inertial actuator, the control system absorbs power from the structure in the frequency range above the actuator resonance; but, below the resonance, control force and structure velocity are in phase, and therefore power is pumped into the structure by the actuator. For large values of feedback gain, the rate of the growth of the power pumped into the structure overtakes the rate of growth of the power absorbed above the actuator resonance, and this explains the reduction in the time-averaged power absorbed beyond the maximum.

Instability has been noticed above the 40% of the gain limit, due to the stroke saturation of the inertial actuator.

Having noticed in Fig. 6 that the control has no effect at high frequency, a second estimation of the time-averaged power absorbed is carried out considering only the first three modes, up to 150 Hz. The force and the velocity signals are filtered with a low-pass second-order Butterworth filter.

From the comparison between the blue and the red line in Fig. 7, it can be noticed that the maximum is more pronounced when a finite frequency range is considered. This is due to the fact that higher structural modes cannot be controlled, as shown in Fig. 6, and therefore they represent a constant term in the time-averaged power absorbed, which reduces the effectiveness of the control system. From this point of view, the evaluation of the time-averaged power absorbed only in the low-frequency range is more attractive, since a sharper behaviour is present. This can result in a more stable implementation of an adaptive control system, which self-tunes the feedback gain in such a way that the power absorbed is maximised.

Finally, the comparison between Fig. 6 and Fig. 7 shows that, for small values of feedback gain, great reduction of the local velocity and increment in the power absorbed can be achieved. Conversely, for high values of feedback gain, the power absorbed slightly decreases. Moreover, a small further reduction in the mobility at the structural resonances corresponds to a large increment of the mobility around the actuator resonance.

5. Conclusions

This paper has presented the experimental control of a structure with a local feedback control system, performed through an inertial actuator.
The conditional stability of the system has been determined according to the Nyquist criterion, analysing the single contribution of each part of the feedback loop. In particular, the stability limit mainly depends on the choice of the inertial actuator and the sampling frequency of the digital controller. Because of these two aspects, the open-loop FRF has a negative real part both in the low-frequency range below the resonance of the actuator, and in the high frequency range due to the delay introduced by the sample-and-hold of the digital controller.
Increasing the feedback gain, large reductions can be obtained on the first resonances, up to 30 dB. Moreover, the local time-averaged power absorbed by the actuator from the structure has been evaluated, so that an optimal gain is found. Finally, according to previous studies, it is believed that the time-averaged power absorbed represents a reliable estimator of the global performance of the control system. The future work will be committed to the estimation of the time-averaged kinetic energy of the structure, and the implementation of a self-tuning control system.

6. Acknowledgements

This research work was supported by the European Commission as “Marie Sklodowska-Curie Fellowship for Early Stage Research” program through the “Initial Training Network” (ITN) within the seventh framework “Advanced Training and Research in Energy Efficient Smart Structures” (ANTARES) project (Grant Agreement 606817).

REFERENCES

1. Elliott, S., Serrand, M. and Gardonio, P. Feedback stability limits for active isolation systems with reactive and inertial actuators, *Journal of Vibration and Acoustics*, **123** (2), 250–261, (2001).

2. Camperi, S., Ghanchi-Tehrani, M., Zilletti, M. and Elliott, S. Multichannel decentralised feedback control using inertial actuators, *Proceedings of the 27th International Conference on Noise and Vibration Engineering, ISMA*, (2016).

3. Elliott, S., Zilletti, M. and Gardonio, P. Self-tuning of local velocity feedback controllers to maximise power absorption, *Recent Advances Structural Dynamics: Proceedings of the X International Conference*, p. 12pp, University of Southampton, (2010).

4. Zilletti, M., Elliott, S. J., Gardonio, P. and Rustighi, E. Experimental implementation of a self-tuning control system for decentralised velocity feedback, *Journal of Sound and Vibration*, **331** (1), 1–14, (2012).

5. Wilmshurst, L. I., *Analysis and control of nonlinear vibration in inertial actuators*, Ph.D. thesis, University of Southampton, (2015).

6. Elliott, S. J. and Zilletti, M. Scaling of electromagnetic transducers for shunt damping and energy harvesting, *Journal of Sound and Vibration*, **333** (8), 2185–2195, (2014).

7. Camperi, S., Ghanchi-Tehrani, M., Zilletti, M. and Elliott, S. Active vibration control of an inertial actuator subject to broadband excitation, *Journal of Physics: Conference Series*, vol. 744, p. 012038, IOP Publishing, (2016).